processes

*Article*

# Optimization of Liquid Phase Catalytic Exchange Process for Hydrogen Isotope Separation Using Orthogonal Experiment Design

**Jingwei Hou, Jiamao Li, Chengjian Xiao, Heyi Wang, Hongwen Huang and Shuming Peng ***

Institute of Nuclear Physics and Chemistry, China Academy of Engineering Physics, Mianyang 621900, China; houjingwei@caep.cn (J.H.)
* Correspondence: pengshuming_2008@163.com

**Abstract:** The Liquid Phase Catalytic Exchange (LPCE) process plays a pivotal role in the separation of hydrogen isotopes, particularly in applications such as tritium removal in heavy water reactors. Effective separation is crucial for maintaining reactor safety and efficiency. In this study, the optimal operating conditions for the LPCE process were determined through orthogonal experiments and validated in different hydrogen isotope systems. The experiments investigated key operational parameters, including the filling ratio of catalyst to packing (FR), operating temperature (T), superficial gas velocity (V), and gas-to-liquid flow rate ratio (λ), using a robust $L_{16}$ orthogonal experiment design. The results indicated that V and FR had the most significant effects on the height equivalent to a theoretical plate (HETP), while λ exhibited the greatest impact on dedeuterization efficiency (DE). The optimal conditions obtained were V = 0.1 m/s, FR = 1:2, T = 70 °C, and λ = 2.5. Furthermore, the reproducibility of the optimal conditions was verified in LPCE columns with varying diameters (1.5 cm, 2.5 cm, 4.5 cm). Additionally, the findings were applied to both H-D and D-T separation systems, demonstrating consistency in mass transfer efficiency and validating the applicability of the optimal conditions in different hydrogen isotope separations. This research provides critical insights for optimizing tritium removal systems in heavy water reactors, contributing to enhanced reactor safety and performance.

**Keywords:** LPCE process; orthogonal experiment; hydrogen isotope separation; tritiated heavy water



**Citation:** Hou, J.; Li, J.; Xiao, C.; Wang, H.; Huang, H.; Peng, S. Optimization of Liquid Phase Catalytic Exchange Process for Hydrogen Isotope Separation Using Orthogonal Experiment Design. *Processes* **2024**, *12*, 2549. https://doi.org/10.3390/pr12112549

Academic Editor: Paola Ammendola

Received: 9 October 2024
Revised: 7 November 2024
Accepted: 13 November 2024
Published: 14 November 2024



## 1. Introduction

Tritium, as a radioactive isotope, is inevitably produced and released in the nuclear energy sector, particularly during the operation of heavy water reactors [1,2]. With a relatively long half-life of 12.3 years, tritium's presence in the environment poses potential hazards to both ecosystems and human health [3]. Therefore, effectively managing and controlling the accumulation and release of tritium has become a critical issue that demands urgent attention in the nuclear energy field [4].

Currently, the primary source of tritium is generated from the operation of fission reactors. For instance, in CANDU heavy water reactors, tritium is produced gradually through the D(n, γ)T reaction between deuterium and neutrons [5]. Over time, this reaction leads to a dynamic equilibrium between the generation and decay of tritium as reactor operations continue. However, due to the radioactive nature of tritium, its accumulation in heavy water not only poses a threat to the safe operation of reactors but also risks environmental contamination through potential leaks. Consequently, periodic extraction and separation of tritium from heavy water is necessary to ensure both reactor safety and environmental sustainability [6].

Among the various techniques for tritium extraction from water, the Liquid Phase Catalytic Exchange (LPCE) process has become a mainstream method for tritium removal from heavy water reactors due to its simple process flow, mild operating conditions, and high

separation efficiency [7]. Several countries, including Russia [8], South Korea [9], and Romania [10], have successfully implemented the LPCE process in their tritium extraction facilities, achieving significant results. For example, South Korea's Wolsong Tritium Removal Facility (WTRF) [9] and Romania's Cernavodă Tritium Removal Facility (CTRF) utilize the LPCE process [10], with tritium removal efficiencies reaching 97% and 98%, respectively.

Despite the promising separation performance of the LPCE process, its engineering application still faces challenges, particularly regarding the excessive height of LPCE columns [11]. Large-scale equipment not only increases construction and maintenance complexity but also imposes higher demands on installation space. Therefore, current research efforts focus on how to reduce equipment height while maintaining high tritium extraction efficiency, improving overall operability and economic feasibility.

To enhance the catalytic efficiency of LPCE columns, two feasible approaches are optimizing materials and refining operating conditions. Previous studies have shown that optimizing catalyst materials—such as the selection of active components, control of particle size and distribution, and choice of support materials—can significantly improve the separation efficiency of LPCE columns [12]. For instance, novel catalytic materials like SDB, carbon black, nickel foam, and SBA-15 have demonstrated excellent tritium separation performance in experiments [13–16]. However, these materials still face challenges in terms of durability and cost in practical applications, necessitating further research.

In addition to material optimization, optimizing operating conditions is also crucial. Parameters such as operating temperature, gas–liquid ratio, gas flow rate, and the packing ratio of catalysts and fillers all have significant impacts on tritium separation efficiency [17]. Traditional single-factor experimental methods are often inefficient and may overlook interactions between different factors. Therefore, in this study, an orthogonal experimental design was employed to systematically optimize key operating parameters in the LPCE process. This design allowed for the efficient evaluation of multiple factors simultaneously, minimizing experimental trials while ensuring that each factor's independent effect was accurately assessed. By using an orthogonal array, this approach guaranteed the balanced distribution of factors and their independent evaluation, reducing interference from factor interactions. To improve optimization efficiency and reduce experimental complexity, an $L_{16}(4^4)$ orthogonal array was employed, enabling the systematic analysis of key parameters. The influence of each parameter on the performance of the LPCE column was analyzed, ensuring the identification of the optimal parameter combination with enhanced experimental efficiency and statistical robustness. This research provides important data support and theoretical guidance for the design of cost-effective tritium removal systems in small-scale research reactors.

## 2. Experimental Section

### *2.1. LPCE Process*

In the LPCE process, gas and liquid enter from the bottom and top of the column, respectively, and undergo counter-current contact within the column. The overall isotope exchange process involves two steps: mass transfer between the gas and liquid phases and the catalytic exchange reaction in the gas phase. Taking the removal of deuterium (HDO) from water as an example, HDO flows in from the top of the column, while $H_2$ enters from the bottom. The reversible reactions are as follows [18]:

$$HDO_{(l)} + H_2O_{(v)} \rightleftarrows H_2O_{(l)} + HDO_{(v)} \quad (1)$$

$$HDO_{(v)} + H_{2(g)} \rightleftarrows H_2O_{(v)} + HD_{(g)} \quad (2)$$

$$HDO_{(l)} + H_{2(g)} \rightleftarrows H_2O_{(l)} + HD_{(g)} \quad (3)$$

Equation (1) represents the mass transfer process between the gas and liquid phases occurring at any gas–liquid interface. Equation (2) describes the catalytic exchange reaction taking place at the active sites of the hydrophobic catalyst. The overall LPCE process is depicted in Equation (3).

### *2.2. Performance Testing of the LPCE Column*

#### 2.2.1. LPCE Apparatus

A schematic diagram of the LPCE apparatus is shown in Figure 1. The system primarily consisted of a top condenser, a catalytic exchange column, a gas pre-treatment unit, and corresponding flow, temperature, and pressure control instruments. The top condenser, catalytic exchange column, and gas pre-treatment unit were all made of glass. The inside of the column was packed with a mixture of 33 cm high stainless-steel spiral–prismatic random packings of 2 mm in size and Pt/SDB hydrophobic catalyst particles of 1–1.2 mm. Additionally, approximately 4 cm of spiral–prismatic random packings were placed at both ends of the column to facilitate gas and liquid distribution and preheating. The flow rates of the feed gas and liquid were precisely regulated by a gas mass flow controller (Sierra, Smart-Trak 2 Model 100, Sierra Instruments, Monterey, CA, USA) and a peristaltic pump (Longer, Model L100-1FS, Langge Constant Flow Pump Co., Ltd., Baoding, China), respectively. A recirculating heater (Huber, Model CC-205B, Peter Huber Kältemaschinenbau, Offenburg, Germany) was employed to maintain a stable temperature within the LPCE column. The deuterium content in the hydrogen isotopic gas sampled from the top of the column was analyzed using gas chromatography (Agilent, Model 7890B, Agilent Technologies, Inc., Santa Clara, CA, USA).

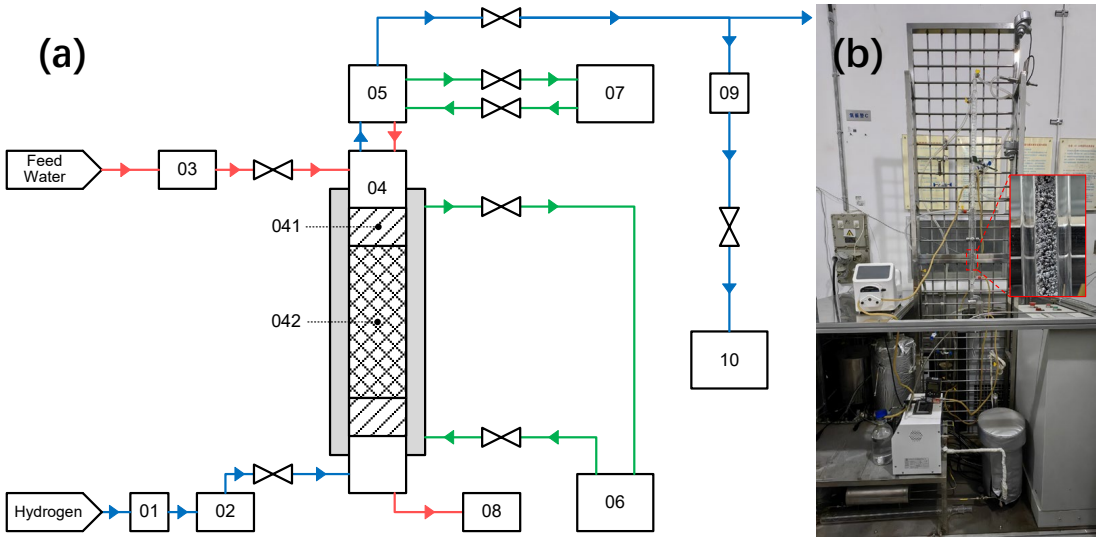


| | |
|---|---|
| 01 Mass flow controller | 05 Condenser |
| 02 Humidifier | 06 Thermostatic circulator |
| 03 Peristaltic pump | 07 Coolant circulator |
| 04 LPCE column | 08 Water tank |
| 041 Spiral–prismatic packing | 09 Dryer |
| 042 Mixed catalytic layer | 10 Gas chromatography |

**Figure 1.** (**a**) Schematic diagram of the LPCE apparatus and (**b**) photo of the experimental setup.

#### 2.2.2. Performance Testing and Calculation of the LPCE Column

The performance testing of the LPCE column was divided into three parts. First, optimal operating conditions were obtained using an orthogonal experiment based on the hydrogen–deuterium system. Second, the effect of scale-up on separation performance was studied by replacing the LPCE column with different diameters under optimal operating conditions. Finally, the tritium removal performance of the LPCE column for heavy water was validated using deuterium–tritium experiments in optimized conditions.

In the orthogonal experiment and scale-up studies, the feed liquid was deuterium-enriched water, specifically prepared to achieve a deuterium abundance of approximately 5%. This was done by carefully mixing deionized water with high-purity $D_2O$ (99.9 atom% D)

under controlled conditions to ensure the uniform distribution of deuterium. The feed liquid entered from the top of the LPCE column, and its flow rate was precisely controlled using a peristaltic pump to ensure an accurate gas–liquid ratio. The peristaltic pump was calibrated using the gravimetric method to verify the flow rate before use.

The feed gas used in the experiment was natural hydrogen. Before entering the LPCE column, the hydrogen gas underwent pre-treatment to adjust its temperature and humidity. Specifically, the gas was preheated to match the reaction temperature inside the column and humidified to the saturated vapor pressure at this temperature. This process was achieved by passing the hydrogen gas through a gas pre-treatment unit equipped with a humidification chamber, where the gas mixed with water vapor to reach saturation. The pre-treated hydrogen gas was then introduced from the bottom of the LPCE column, moving counter-currently to the downward-flowing deuterium-enriched water. The gas flow rate was controlled using a mass flow controller, which was calibrated with a soap film flowmeter.

Inside the LPCE column, the counter-current contact between the deuterium-enriched water and hydrogen gas facilitated the hydrogen isotope exchange reaction, involving the transfer of deuterium atoms from the water molecules to the hydrogen gas molecules. The column temperature was maintained at a constant level using a recirculating heater.

The hydrogen gas exiting the LPCE column contained deuterium. After undergoing cryogenic separation to remove residual water vapor, dry hydrogen gas was obtained. This process involved cooling the hydrogen gas to liquid nitrogen temperature, causing the water vapor to condense and separate out. The processed hydrogen gas was then directed to a gas chromatograph (Agilent, 7890B) for the precise measurement of deuterium concentration.

The performance of the LPCE column was evaluated in terms of the height equivalent to a theoretical plate (HETP) and dedeuterization efficiency (DE), which were calculated using Equations (4)–(6) [19].

$$\mathrm{HETP} = \frac{h}{\mathrm{NTU}} \cdot \frac{\ln\left(\frac{\alpha}{\lambda}\right)}{1 - \frac{\alpha}{\lambda}} \tag{4}$$

$$\mathrm{NTU} = \frac{y_b - y_t}{\left(y_b - y_b^*\right) - \left(y_t - y_t^*\right)} \cdot \ln \frac{y_b - y_b^*}{y_t - y_t^*} \tag{5}$$

$$\mathrm{DE} = 1 - \frac{x_b}{x_t} = 1 - \frac{x_t - (y_t - y_b) \cdot \lambda}{x_t} \tag{6}$$

where HETP is the height equivalent to a theoretical plate; h is the height of the packing layer; NTU represents the number of theoretical stages; $\alpha$ is the separation factor; $\lambda$ is the gas–liquid ratio; $y_b$ and $y_t$ represent the deuterium abundance in the gas phase at the bottom and top of the column, respectively; $x_b$ and $x_t$ represent the deuterium abundance in the liquid phase at the bottom and top of the column, respectively; and $y_b^*$ and $y_t^*$ represent the deuterium abundance in the gas phase at the bottom and top of the column at equilibrium. The separation factor $\alpha$ was calculated using Equation (7) [19].

$$y^* = \frac{x}{\alpha - x \cdot (\alpha - 1)} \tag{7}$$

After determining the optimal conditions from the orthogonal experiment, single-factor experiments were conducted to validate these conditions across different column diameters and hydrogen isotope systems, using temperature as the variable. The column diameters were 1.5 cm, 2.5 cm, and 4.5 cm. Validation tests were performed in both DTO and $D_2$ hydrogen isotope systems, utilizing catalytic exchange reactions to assess the performance under varying conditions.

### 2.3. Orthogonal Experimental Design and Analysis Method

The orthogonal experimental method is a design approach used to study multiple factors and levels. It selects an appropriate number of representative test cases from a large amount of test data characterized by uniform distribution and neat comparability [20]. The design of the orthogonal experiment was based on orthogonal arrays. In this study,

the factors were the parameters affecting the performance of the LPCE column, while the levels referred to the number of different conditions for each factor. Thus, the orthogonal experiment was designed to optimize the parameters of the LPCE column, which involved multiple variables and multiple levels.

To improve the hydrogen isotope separation efficiency of the LPCE column, its operating parameters needed to be optimized. With the catalyst and packing materials predetermined, the four main parameters affecting the separation performance of the LPCE column were the filling ratio of catalyst to packing (FR), operating temperature (T), superficial gas velocity (V), and gas to liquid flow rate ratio (λ). The selection of these parameters was informed by both LPCE column design considerations and practical application needs. From a design perspective, FR influenced the gas–liquid contact area by adjusting the proportion of catalyst to packing, thereby affecting mass transfer efficiency. Specifically, the chosen levels (1:2 to 1:5) allowed for the systematic assessment of various catalyst quantities to identify the optimal filling ratio for efficient separation. T affected reaction rate and catalyst activity and the chosen temperature range (50 °C to 80 °C) encompassed the optimal operating conditions for the LPCE column, enabling comparison under different thermodynamic conditions. V determined the dynamics of mass transfer at the gas–liquid interface and the set levels (10 cm/s to 25 cm/s) covered a range from low to high velocities to assess its effect on gas–liquid contact time and separation efficiency. λ affected the equilibrium state of gas–liquid interaction; levels from 1 to 2.5 provided varying relative flow conditions, aiding the analysis of how the flow rate ratio influenced isotope exchange efficiency. Each of these factors was essential in balancing performance and cost-effectiveness, requiring precise optimization in the design phase.

To conduct the experiments more efficiently, each factor was set at four levels, with specific values shown in Table 1. If traditional methods had been used, $4^4$ experiments would have been required to study the influence of these parameters on the LPCE column's performance. To reduce the number of experiments and improve optimization efficiency, the orthogonal experiment method was adopted. This method ensures a uniform combination of test factors and levels, achieving both uniformity and comparability, making it an efficient experimental design approach.

**Table 1.** The factors and levels of the orthogonal experiment.

| Level *i* | Factors | | | |
|---|---|---|---|---|
| | **FR (*j* = 1)** | **T (°C) (*j* = 2)** | **V (cm/s) (*j* = 3)** | **λ (*j* = 4)** |
| 1 | 1:2 | 80 | 10 | 1 |
| 2 | 1:3 | 70 | 15 | 1.5 |
| 3 | 1:4 | 60 | 20 | 2 |
| 4 | 1:5 | 50 | 25 | 2.5 |

To optimize the operating parameters of the LPCE column, an $L_{16}(4^4)$ orthogonal experiment was designed, as shown in Table 2. The separation performance of the LPCE column under each set of parameters was obtained through hydrogen–water isotope exchange experiments and the orthogonal array was used to evaluate the influence of each factor on the performance of the LPCE column.

**Table 2.** The orthogonal experiment design table.

| Exp. Number | Factors | | | |
|---|---|---|---|---|
| | **FR (*j* = 1)** | **T (°C) (*j* = 2)** | **V (cm/s) (*j* = 3)** | **λ (*j* = 4)** |
| 1 | 1:2 | 80 | 10 | 1 |
| 2 | 1:2 | 70 | 15 | 1.5 |

**Table 2.** *Cont.*

| Exp. Number | Factors | | | |
|---|---|---|---|---|
| | FR ($j$ = 1) | T (°C) ($j$ = 2) | V (cm/s) ($j$ = 3) | λ ($j$ = 4) |
| 3 | 1:2 | 60 | 20 | 2 |
| 4 | 1:2 | 50 | 25 | 2.5 |
| 5 | 1:3 | 80 | 15 | 2 |
| 6 | 1:3 | 70 | 10 | 2.5 |
| 7 | 1:3 | 60 | 25 | 1 |
| 8 | 1:3 | 50 | 20 | 1.5 |
| 9 | 1:4 | 50 | 20 | 2.5 |
| 10 | 1:4 | 70 | 10 | 2 |
| 11 | 1:4 | 60 | 25 | 1.5 |
| 12 | 1:4 | 80 | 15 | 1 |
| 13 | 1:5 | 50 | 10 | 1.5 |
| 14 | 1:5 | 70 | 20 | 1 |
| 15 | 1:5 | 60 | 15 | 2.5 |
| 16 | 1:5 | 80 | 25 | 2 |

#### 2.3.1. Range Analysis

Range analysis is a statistical method used to evaluate the significance of factor effects based on the range of average response values for the target effect [21]. It helps to determine the sensitivity of each factor to the experimental results through orthogonal experiments. The larger the range, the more sensitive the factor is.

Based on the target effect values obtained at each level of the factors, the total response value $K_{ij}$ and the average response value $k_{ij}$ at each level of the factors were calculated.

Equation (8) was derived from the target response values obtained at each level of the factors and utilized to calculate the total response value $K_{ij}$ and the average response value $k_{ij}$ at each level. Specifically, $K_{ij}$ represented the sum of target response values at level $i$ of factor $j$. Dividing this total by 4 (corresponding to the four experimental combinations per level) yielded the average response value $k_{ij}$. For instance, for the factor FR, the total response value $K_{11}$ for HETP was determined by summing the results of test numbers 1 to 4, and dividing the sum by 4 produced $k_{11}$. This standardization facilitated the comparison of response values across different levels.

$$k_{ij} = \frac{K_{ij}}{4} \tag{8}$$

Equation (9) provides the method for calculating the range $R_j$ of the average response values for each factor, defined as the difference between the maximum average response value $k_{max,j}$ and the minimum average response value $k_{min,j}$ across different levels of the same factor. This range was obtained by subtracting $k_{min,j}$ from $k_{max,j}$. A larger $R_j$ indicated that the factor exerted a more significant influence on the target response.

$$R_j = k_{max,j} - k_{min,j} \tag{9}$$

where $i$ represents the level number ($i$ = 1, 2, 3, 4) and $j$ represents the factor number ($j$ = 1, 2, 3, 4).

#### 2.3.2. Analysis of Variance (ANOVA)

In the orthogonal design table, since there was no blank column, the performance prediction values for each experimental condition were fitted using the method of linear regression. Based on this, the residuals were calculated. Subsequently, the sum of squares for error (SSE), degrees of freedom for error (DFE), and mean square error (MSE) were computed.

Taking HETP as an example, to quantify the influence of each factor on HETP, a multivariate linear regression analysis was performed on the experimental data using the Ordinary Least Squares (OLS) method. The expression of the linear regression model was as follows:

$$\mathrm{HETP} = \beta_0 + \beta_1 \times \mathrm{FR} + \beta_2 \times \mathrm{T} + \beta_3 \times \mathrm{V} + \beta_4 \times \lambda + \epsilon \tag{10}$$

where $\beta_0$ is the intercept term, $\beta_1$ to $\beta_4$ represent the regression coefficients for each factor, and $\epsilon$ is the error term. The optimal values for the regression coefficients were estimated by minimizing the sum of squared residuals between the observed and predicted values.

Based on the regression coefficients estimated from the linear regression model, an ANOVA was performed on the experimental data to assess the significance of each factor's influence on HETP. First, the mean square (MS) for each factor and the mean square error (MSE) were calculated, followed by an F-test to determine the significance level of each factor. The formulas for calculating the sum of squares for error (SSE) and degrees of freedom for error (DFE) are provided below:

$$\mathrm{SSE} = \sum_{i=1}^{n} \left(Y_i - \hat{Y}_i\right)^2 \tag{11}$$

$$\mathrm{MSE} = \frac{\mathrm{SSE}}{\mathrm{DFE}} \tag{12}$$

where $n$ is the number of observations, $Y_i$ is the observed value of the dependent variable for the i observation, and $\hat{Y}_i$ is the predicted value of the dependent variable for the i observation.

In this study, there were 16 data sets, and the degrees of freedom for each factor equaled 3, resulting in an error degree of freedom (DFE) of 3. The calculated mean square error (MSE) was 0.548. The F-value for each factor was calculated using the following formula:

$$\mathrm{F} = \frac{\mathrm{MS}_{\mathrm{factor}}}{\mathrm{MSE}} \tag{13}$$

$\mathrm{MS}_{\mathrm{factor}}$ represents the mean square of the factor, which quantifies the variation it contributes to the response variable. The MSE, computed as 0.548, reflected the residual variation not explained by the model. The F-value thus served as a metric to assess the relative impact of each factor compared to experimental error.

A higher F-value suggested a more pronounced effect of the factor on the target response. By comparing the calculated F-value to the critical value at a predetermined significance level, the statistical significance of each factor could be assessed. If the F-value surpassed the critical threshold, the factor was deemed significant, indicating a substantial influence on the HETP.

Equation (13) thereby provided a systematic approach for identifying which factors exhibited statistically significant effects, contributing to the interpretation of the experimental data and guiding further process optimization.

The variance analysis method for DE was the same as that for HETP.

## 3. Results and Discussion

### *3.1. Analysis of Orthogonal Test Results*

A total of 16 experiments were conducted in the orthogonal tests, with results for HETP and DE under each experimental condition summarized in Table 3. The results indicate that Experiment 6 yielded the optimal HETP, while Experiment 7 demonstrated the least effectiveness. For DE, Experiment 6 also achieved the highest value, whereas Experiment 14 exhibited the lowest.

**Table 3.** The results of the L16 orthogonal experiment.

| Exp. Number | HETP | DE |
|---|---|---|
| 1 | 11.51 | 0.34 |
| 2 | 10.64 | 0.45 |
| 3 | 12.28 | 0.57 |
| 4 | 15.54 | 0.58 |
| 5 | 17.41 | 0.53 |
| 6 | 10.30 | 0.67 |
| 7 | 22.09 | 0.29 |
| 8 | 18.79 | 0.39 |
| 9 | 18.78 | 0.55 |
| 10 | 10.51 | 0.57 |
| 11 | 21.27 | 0.40 |
| 12 | 20.40 | 0.31 |
| 13 | 13.05 | 0.42 |
| 14 | 21.26 | 0.28 |
| 15 | 13.76 | 0.64 |
| 16 | 21.96 | 0.49 |

#### 3.1.1. Range Analysis Results

The average response values $k_{ij}$ and the range $R_j$ for the four key factors (FR, T, V, and λ) affecting HETP and DE at different levels were calculated from the orthogonal test results. The findings are presented in Table 4.

**Table 4.** The value of $k_{ij}$ and R for HETP and DE.

| | HETP (cm) | | | | DE | | | |
|---|---|---|---|---|---|---|---|---|
| | **FR ($j$ = 1)** | **T ($j$ = 2)** | **V ($j$ = 3)** | **λ ($j$ = 4)** | **FR ($j$ = 1)** | **T ($j$ = 2)** | **V ($j$ = 3)** | **λ ($j$ = 4)** |
| $k_{1j}$ | 12.49 | 16.54 | 11.34 | 18.81 | 0.487 | 0.484 | 0.500 | 0.304 |
| $k_{2j}$ | 17.15 | 13.18 | 15.55 | 15.94 | 0.470 | 0.494 | 0.483 | 0.414 |
| $k_{3j}$ | 17.74 | 17.35 | 17.78 | 15.54 | 0.456 | 0.475 | 0.447 | 0.543 |
| $k_{4j}$ | 17.51 | 17.82 | 20.21 | 14.60 | 0.458 | 0.418 | 0.441 | 0.610 |
| $R_j$ | 5.25 | 4.64 | 8.87 | 4.22 | 0.031 | 0.076 | 0.060 | 0.306 |

Influence of Each Factor on HETP

According to the range analysis results in Table 4, the order of factor significance for HETP was $R_3 > R_1 > R_2 > R_4$, meaning that V has the greatest impact on HETP, followed by FR, T, and λ, which had the smallest effect. The optimal operating conditions were determined to be V = 0.1 m/s, FR = 1:2, T = 70 °C, and λ = 2.5. To more clearly illustrate the effects of the various factors on HETP, a trend graph was plotted using the range analysis data from Table 4, with the factor levels on the x-axis and HETP's $k_{ij}$ values on the y-axis, as shown in Figure 2.

HETP directly reflected the mass transfer efficiency and separation performance of the catalytic exchange column. As shown in the figure, when V was at its lowest, the HETP value was minimized, indicating that under the experimental conditions, mass transfer efficiency was optimal at this gas velocity. With increasing V, the HETP increased significantly. This phenomenon could be attributed to the longer residence time of the gas phase in the packed column at lower velocities, allowing more thorough mass transfer and hydrogen isotope exchange [22]. In the LPCE column, the liquid adhered to the packing surface, forming a liquid film that served as the primary interface for gas–liquid mass transfer. Under fully wetted conditions, the effective gas–liquid mass transfer area was largely determined by the specific surface area of the packing, and, therefore, increases in gas or liquid flow rates had a limited impact on the mass transfer area. However, as

the gas velocity increased, the contact time between the gas and liquid, as well as the interaction time between the gas phase and the catalytic active sites, significantly decreased, thus limiting effective mass transfer. Additionally, reduced contact time was unfavorable for sufficient hydrogen isotope exchange, leading to a notable decline in mass transfer efficiency, ultimately manifesting as an increase in HETP with increasing gas velocity.

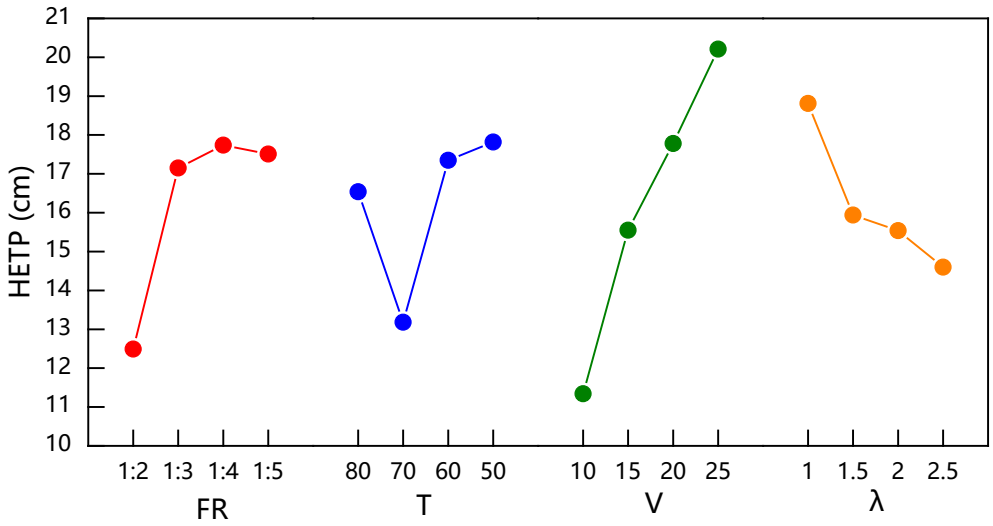


**Figure 2.** Single-factor influence trend based on range analysis of HETP.

The FR also had a significant impact on HETP. When FR was 1:2, a higher packing ratio provided a sufficient gas–liquid interface and adequate catalyst availability, ensuring efficient hydrogen isotope exchange in the gas phase and reducing mass transfer resistance. As FR decreased, although the amount of packing increased, thereby expanding the mass transfer area, the reduction in catalyst quantity led to a decrease in the isotope exchange rate, resulting in lower mass transfer efficiency and a sharp increase in HETP. Further reductions in FR, despite the continued increase in gas–liquid interface area, did not lead to a significant reduction in HETP due to insufficient reaction rates to support effective mass transfer. Therefore, the influence of FR on HETP reflected the balance between gas–liquid mass transfer and catalytic reaction.

The effects of T and λ were relatively weaker compared to FR. Temperature affected both the equilibrium constant of the reaction and the water vapor content in the gas phase. With an increase in temperature, the equilibrium constant increased, which favored the conversion of HDO. However, the water vapor content in the gas phase also increased significantly. The former promoted HDO conversion, whereas the latter diluted the hydrogen, reducing its interaction with the active sites and thereby lowering the hydrogen isotope exchange efficiency. Additionally, the increase in water vapor content led to an increase in the overall gas flow, resulting in a higher gas velocity, which was unfavorable for the LPCE process. Considering these factors, the performance was optimal at 70 °C. The influence of λ was minimal compared to other factors. As seen in Equation (4), the effect of the gas–liquid ratio on HETP was accounted for in the calculation, providing a standardized indicator of mass transfer performance, which resulted in λ having the least impact among the four factors.

Influence of Each Factor on DE

From the data presented in Table 4, the range values for DE indicate that the order of influence was $R_4 > R_2 > R_3 > R_1$, which means that under the combined influence of multiple factors, the significance of each factor affecting DE was in the order λ > T > V > FR. The optimal operating conditions were FR = 1:2, T = 70 °C, V = 0.1, and λ = 2.5. Similarly, a trend graph was plotted using the range analysis data from Table 4, as shown in Figure 3, with the levels of different factors as the horizontal axis and $k_{ij}$ values of DE as the vertical axis.

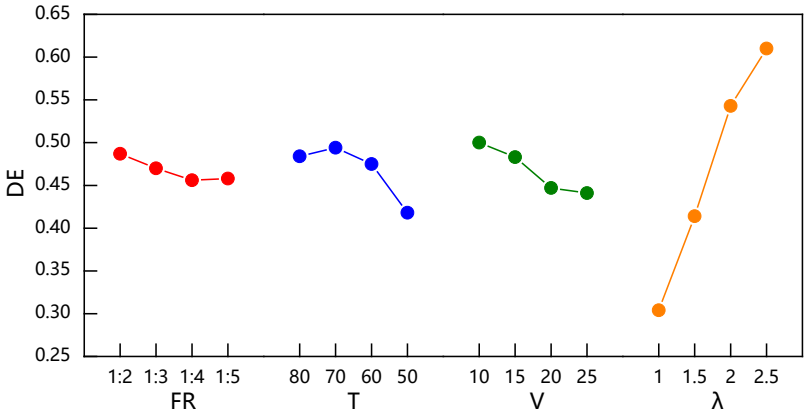


**Figure 3.** Single-factor influence trend based on range analysis of DE.

DE intuitively reflected the ability of the LPCE column to remove hydrogen isotope components under various operating conditions. As shown in the figure, the influence of the λ was significantly greater than that of the other factors. With the increase in λ, DE increased substantially, which was likely due to the increased hydrogen concentration in the gas phase, providing more reactants for hydrogen isotope exchange, thereby enhancing the efficiency of the isotopic exchange. Particularly at higher λ values, deuterium in the liquid phase was more readily transferred to the gas phase, resulting in a higher removal rate. Thus, the increase in λ directly improved the deuterium conversion efficiency, leading to a notable enhancement in DE.

Temperature had the second-largest impact on DE. Temperature affected both the equilibrium constant and the reaction kinetics. An optimal temperature (e.g., 70 °C) could simultaneously enhance the equilibrium constant and reaction rate, achieving the most effective hydrogen isotope conversion efficiency. However, excessively high temperatures led to increased water vapor content in the gas phase, diluting the hydrogen concentration, which inhibited the isotopic exchange process.

The V on DE was secondary to λ and temperature. Lower gas velocities helped extend the contact time between the gas and liquid phases, improving the completeness of isotopic exchange and thereby enhancing DE. However, as the gas velocity increased, the contact time between phases was significantly reduced, which limited mass transfer and decreased hydrogen isotope exchange efficiency, resulting in a decline in DE.

The FR on DE was minimal. Although increasing the packing ratio could expand the gas–liquid mass transfer interface, the overall reaction efficiency was primarily influenced by other factors, such as λ and temperature. Once the packing ratio reached a sufficient level, further increases had a negligible effect on DE. This was because the mass transfer interface area reached a saturation point, and additional increases contributed minimally to the reaction rate.

### 3.1.2. Results of ANOVA

The experimental data were analyzed using the analysis of variance method, and the results for HETP and DE are presented in Tables 5 and 6, respectively.

**Table 5.** ANOVA results for HETP.

| Factor | SS | df | MS | F | *p* |
|---|---|---|---|---|---|
| FR | 74.89 | 3 | 24.96 | 45.57 | 0.0053 |
| T | 16.73 | 3 | 5.58 | 10.18 | 0.0442 |
| V | 136.11 | 3 | 45.37 | 82.81 | 0.0022 |
| λ | 26.26 | 3 | 8.75 | 15.98 | 0.0238 |
| Residual | 1.64 | 3 | 0.548 | / | / |

**Table 6.** ANOVA results for DE.

| Factor | SS | df | MS | F | *p* |
|---|---|---|---|---|---|
| FR | 0.00205 | 3 | 0.000683 | 2.14 | 0.2742 |
| T | 0.00484 | 3 | 0.001614 | 5.05 | 0.1082 |
| V | 0.00773 | 3 | 0.002576 | 8.07 | 0.0601 |
| λ | 0.19983 | 3 | 0.066611 | 208.52 | 0.0006 |
| Residual | 0.00096 | 3 | 0.000319 | / | / |

Table 5 presents the ANOVA results for the impact of different factors on the height equivalent to a theoretical plate (HETP) in the LPCE column, including the effects of the filling ratio (FR), temperature (T), superficial gas velocity (V), and gas–liquid flow rate ratio (λ). The analysis covered each factor's sum of squares (SS), degrees of freedom (df), mean squares (MS), F-value, and *p*-value. The results indicate that V had the most significant effect on HETP, with an SS of 136.11, an F-value of 82.81, and a *p*-value of 0.0022, which was far below 0.05. This highlights the strong statistical significance of V, underscoring its critical influence on HETP due to its direct impact on gas–liquid contact time and mass transfer dynamics. FR also showed a significant effect on HETP, with an F-value of 45.57 and a *p*-value of 0.0053, indicating its importance within the experimental conditions. FR affected mass transfer efficiency by altering the ratio of catalyst to packing material, thus making it a relevant factor for process optimization. The F-value for T was 10.18, with a *p*-value of 0.0442, demonstrating statistical significance at the 0.05 level, albeit to a lesser extent than V and FR, suggesting that changes in T had a moderate impact on HETP. The F-value for λ was 15.98, with a *p*-value of 0.0238, indicating statistical significance but a lower impact compared to V and FR. λ affected the equilibrium state of gas–liquid interaction and, therefore, indirectly influenced mass transfer performance. The residual sum of squares was 1.64, indicating minimal experimental error and strong model explanatory power. Overall, the ANOVA results reveal that V had the most pronounced effect on HETP, followed by FR, and should be prioritized in the design and optimization of LPCE columns. While T and λ also showed statistical significance, their relative impact was lower.

Overall, the results of the ANOVA align with those from the range analysis, suggesting that in order to improve HETP, priority should be given to adjusting the superficial gas velocity and FR in LPCE columns. However, for systems with a fixed processing capacity, reducing gas velocity typically requires increasing the column diameter and the amount of packing and catalyst, which can lead to higher costs. Although a higher FR can result in lower HETP and allow for a shorter column height to achieve the same separation performance, the amount of catalyst required increases significantly. Since catalyst costs are much higher than those of packing materials, this could also lead to higher capital investments in LPCE columns, reducing their economic viability.

In practical applications, the choice of operating parameters must be made based on the specific requirements. If economic considerations are the primary concern, a lower FR should be employed. However, in situations where height limitations are a critical factor, a higher FR would be necessary to meet performance goals.

As shown in Table 6, the ANOVA results for DE indicate that the gas–liquid flow rate ratio (λ) had the most significant impact on DE, with a sum of squares of 0.19983, an F-value of 208.52, and a *p*-value of 0.0006, which was far below the 0.05 significance level. This demonstrates its high statistical significance, suggesting that changes in λ substantially affected DE due to its direct influence on the availability of hydrogen for the isotope exchange process. The F-value for superficial gas velocity (V) was 8.07, with a *p*-value of 0.0601, which did not meet the 0.05 significance threshold but indicated that V had a potential influence on DE, being close to statistical significance. This suggests that within the experimental range, increasing or adjusting V may have an impact on DE. The F-value for temperature (T) was 5.05, with a *p*-value of 0.1082, indicating that T did not have a statistically significant effect on DE under the current experimental conditions. The

F-value for the filling ratio (FR) was 2.14, with a *p*-value of 0.2742, showing that FR had the smallest impact on DE and was not significant at the 0.05 level. The limited effect of FR may be attributed to its primary role in modulating the gas–liquid contact area, which had a minimal contribution to variations in DE.

The residual sum of squares was 0.00096, indicating minimal experimental error and a strong explanatory power of the ANOVA model. Overall, the results highlight that the gas–liquid flow rate ratio (λ) was the key factor influencing DE, with a significantly greater impact than the other factors. Therefore, optimizing λ should be a priority in the design and operation of LPCE columns. Although V did not meet strict statistical significance, its proximity to the significance level suggests that adjustments to V could be beneficial for improving DE. Temperature (T) and the filling ratio (FR) did not show significant impacts under the current experimental conditions and can be considered secondary factors during optimization.

Similarly, the results of the ANOVA are consistent with those from the range analysis, further confirming the importance of λ as a key operational parameter. By optimizing the gas–liquid ratio, DE can be significantly improved, thereby enhancing the removal efficiency of heavy components. This finding provides important guidance for optimizing the LPCE process, particularly in the efficient separation and purification of deuterium-enriched water, where optimizing the gas-liquid ratio is critical for improving overall process performance.

### *3.2. Validation of Optimal Conditions*

In the existing literature, the optimal parameters for the LPCE process typically include key factors such as the gas–liquid flow rate ratio (λ), superficial gas velocity (V), operating temperature (T), and filling ratio (FR). For example, Li et al. found through single-factor experiments that higher separation efficiency in an LPCE column can be achieved at temperatures between 60 °C and 80 °C and a gas–liquid flow rate ratio between 1.5 and 2.5 [22]. Junhua Li and colleagues demonstrated that under mixed packing conditions, increasing the filling ratio from 1:6 to 1:2 significantly decreased mass transfer performance, with the total mass transfer coefficient dropping from 2.229 to 0.7137. However, under conditions without flooding and with controllable costs, increasing the amount of catalyst could enhance mass transfer efficiency [23]. Fedorchenko et al. reported that lower gas velocities were more favorable for hydrogen–water isotope mass transfer in the LPCE process, noting that as the superficial gas velocity increased from 0.13 m/s to 0.22 m/s, the HETP rose linearly from 23 cm to approximately 34 cm [24].

In our study, we found that the optimal separation performance was achieved within the experimental conditions set at λ = 2.5, T = 70 °C, FR = 1:2, and superficial gas velocity of 10 cm/s. This result differs from some literature findings by indicating that a lower gas velocity provides better HETP values, suggesting that reduced velocity extends the gas–liquid contact time and enhances mass transfer efficiency. While our results align with the trend observed by Fedorchenko et al. [24], our data indicate better performance at a lower gas velocity. Additionally, our experiments confirm that 70 °C is an optimal operating temperature, consistent with Li et al.'s findings [22].

To further validate the reproducibility of the optimal conditions identified in the orthogonal experiment, a single-factor experiment on temperature was further conducted using LPCE columns with diameters of 1.5 cm, 2.5 cm, and 4.5 cm. The experimental conditions were set to V = 0.1 m/s, FR = 1:2, and λ = 2.5 to validate the reproducibility of the optimal conditions. The results are shown in Figure 4. It can be observed that the lowest HETP values for each column diameter appeared around 70 °C, consistent with the trends observed in the orthogonal experiments. When the column diameter was 1.5 cm, the HETP was 8.79 cm, which was lower than that of Experiment 6, confirming that the optimal conditions obtained from the orthogonal analysis were valid.

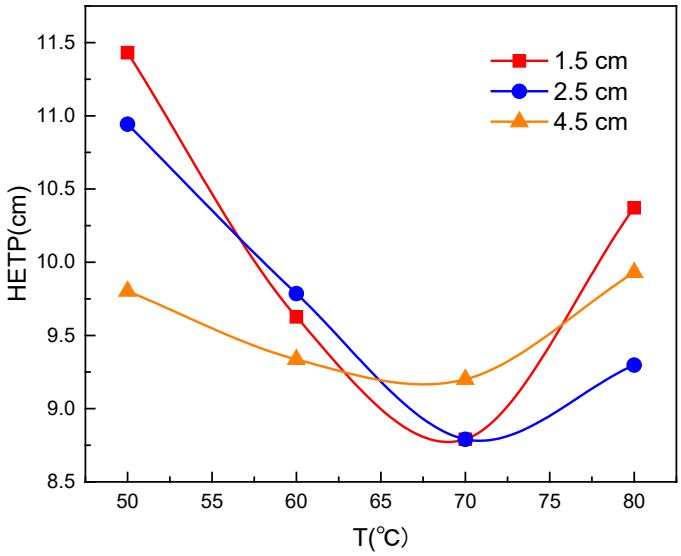


**Figure 4.** Variation of HETP with temperature for different column diameters.

Moreover, the results reveal the effect of column scale-up on the performance of the LPCE column. As the column diameter increased, the amplitude of HETP variation with temperature decreased, indicating that larger column diameters reduced the temperature sensitivity of the LPCE column. This phenomenon may be attributed to the fact that LPCE columns typically employ external heating, and, as the column diameter increases, radial temperature uniformity deteriorates. This leads to a greater deviation between the actual reaction temperature and the set temperature, resulting in the LPCE column operating within a narrower effective temperature range.

This study further validates the applicability of the optimal process conditions across different scales and demonstrates that temperature uniformity must be considered when scaling up the LPCE process. For large-scale equipment, precise radial temperature control will be critical in maintaining high mass transfer efficiency.

Using tritiated heavy water with an activity of $1.47 \times 10^5$ Bq/kg as the feed, the optimal operating conditions were validated in different hydrogen isotope systems, and the results are shown in Figure 5. It can be observed that under optimal conditions, the removal efficiency of heavy components in both the H-D and D-T systems followed a similar trend with temperature, reaching the best performance at 70 °C, consistent with the results of the orthogonal experiments. This verifies the applicability of the optimal conditions obtained from the orthogonal experiments in different isotope systems and confirms the comparability of the experimental results. These findings suggest that the mass transfer behavior in the H-D and D-T systems under similar operating conditions showed good generalizability, allowing the results to be cross-referenced and reducing the need for radioactive experiments.

Additionally, the experimental results show that in the H-D separation process, the removal efficiency of heavy components ranged from 64.5% to 70%, which was significantly lower than in the D-T system. This was mainly due to the limitations of chemical equilibrium, as heavy components in the D-T system more easily transfer to the gas phase. Compared to the H-D system, the D-T system exhibited higher mass transfer efficiency due to the higher molecular mass of tritium.

By comparing different hydrogen isotope systems, this study further enhances the understanding of mass transfer mechanisms in isotope separation, providing critical experimental data and theoretical support for the design and optimization of industrial-scale isotope separation processes. In particular, the higher mass transfer efficiency in the D-T separation process will lay the foundation for the economic viability and efficiency of process scale-up and practical applications.

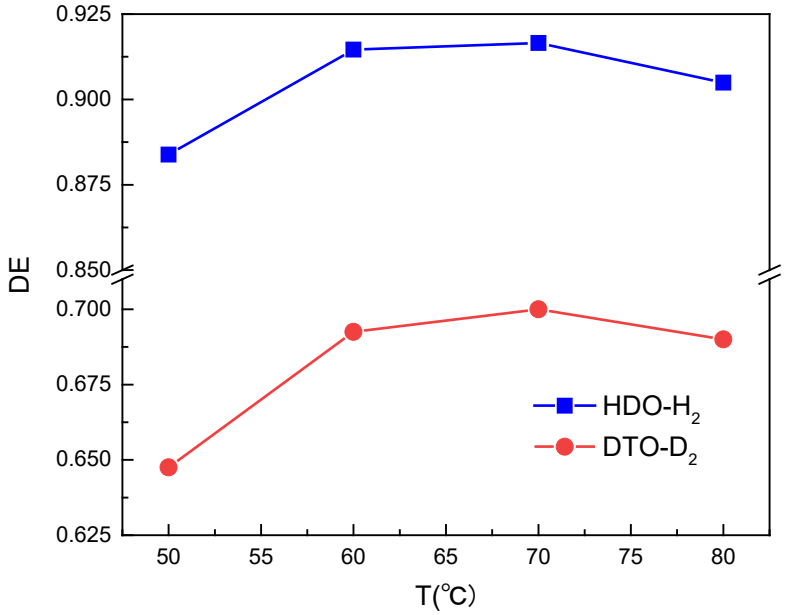


**Figure 5.** Variation of heavy component removal efficiency with temperature.

## 4. Conclusions

This study employed an orthogonal experimental design to optimize the key operational parameters for the LPCE process, including gas velocity, filling ratio, temperature, and gas–liquid ratio. The results demonstrate that the gas velocity and filling ratio are the most influential factors for minimizing HETP, while the gas–liquid ratio has the most significant impact on DE. The optimal operating conditions obtained from the experiments were further validated across different LPCE column diameters, confirming the reproducibility of the results. The temperature sensitivity of the LPCE column was found to decrease as the column diameter increased, suggesting that temperature uniformity should be a key consideration during process scale-up.

Moreover, validation experiments conducted using both H-D and D-T systems showed that the removal efficiency of heavy components followed a consistent trend with temperature, with optimal performance achieved at 70 °C. The comparability of the experimental results between the two systems indicates that the optimal conditions derived from the orthogonal experiments are applicable across different hydrogen isotope separations. This study provides valuable data for improving the LPCE process, particularly the separation and purification of deuterium-enriched water, and offers a foundation for optimizing industrial-scale isotope separation systems.

**Author Contributions:** Conceptualization, S.P.; methodology, J.H. and H.W.; formal analysis, J.L.; resources, C.X. and H.H.; writing—original draft, J.H.; writing—review and editing, J.H.; supervision, S.P. All authors have read and agreed to the published version of the manuscript.

**Funding:** This research received no external funding.

**Data Availability Statement:** The original contributions presented in the study are included in the article, further inquiries can be directed to the corresponding author.

**Conflicts of Interest:** The authors declare no conflict of interest.

## References

1. Jones, G. Tritium issues in commercial pressurized water reactors. *Fusion Sci. Technol.* **2008**, *54*, 329–332. [CrossRef]
2. Bukin, A.N.; Marunich, S.; Pak, Y.; Rastunova, I.; Rozenkevich, M.; Chebotov, A.Y. Specific features and current status of processes for tritium removal from water: A critical review. *Fusion Sci. Technol.* **2022**, *78*, 595–606. [CrossRef]
3. Lu, B.; Yang, X.; Liu, J.; Li, R. Progress on Tritium Toxicity and Detoxification Strategies. *ACS Chem. Health Saf.* **2024**, *31*, 144–152. [CrossRef]

4. Eyrolle, F.; Ducros, L.; Le Dizès, S.; Beaugelin-Seiller, K.; Charmasson, S.; Boyer, P.; Cossonnet, C. An updated review on tritium in the environment. *J. Environ. Radioact.* **2018**, *181*, 128–137. [CrossRef]
5. Park, T.K.; Kim, S.K. Tritium: Its generation and pathways to the environment at CANDU 6 generating stations. *Nucl. Eng. Des.* **1996**, *163*, 405–411. [CrossRef]
6. Vasyanina, T.V.; Alekseev, I.A.; Bondarenko, S.D.; Fedorchenko, O.A.; Konoplev, K.A.; Arkhipov, E.A.; Uborsky, V.V. Heavy water purification from tritium by CECE process. *Fusion Eng. Des.* **2008**, *83*, 1451–1454. [CrossRef]
7. Fedorchenko, O.A.; Alekseev, I.A.; Bondarenko, S.D.; Vasyanina, T.V. Recent progress in the experimental study of LPCE process on "eVIO" pilot plant. *Fusion Sci. Technol.* **2017**, *71*, 432–437. [CrossRef]
8. Bondarenko, S.D.; Alekseev, I.A.; Fedorchenko, O.A.; Vasyanina, T.V. The current status of the heavy water detritiation facility at the NRC (Kurchatov Institute)–PNPI. *Fusion Sci. Technol.* **2020**, *76*, 690–695. [CrossRef]
9. Song, K.M.; Sohn, S.H.; Kang, D.W.; Paek, S.W.; Ahn, D.H. Installation of liquid phase catalytic exchange columns for the Wolsong tritium removal facility. *Fusion Eng. Des.* **2007**, *82*, 2264–2268. [CrossRef]
10. Zamfirache, M.; Bornea, A.; Balteanu, O.; Bucur, C.; Sofilca, N.; Stefanescu, I. Final status of water detritiation system (WDS) for Cernavoda Tritium removal facility (CTRF). *Fusion Eng. Des.* **2018**, *136*, 1038–1040. [CrossRef]
11. Song, K.M.; Lee, S.J.; Lee, S.K.; Sohn, S.H.; Eum, H.M.; Kim, C.-S. The prediction of tritium level reduction of Wolsong NPPs by heavy water detritiation with WTRF. *Fusion Sci. Technol.* **2005**, *48*, 290–293. [CrossRef]
12. Mhd Yusof, S.M.; Lock, S.S.M.; Abdul Talib, N.N.; Seng, L.C. A Mini Review on Liquid Phase Catalytic Exchange for Hydrogen Isotope Separation: Current Status and Future Potential. *Sustainability* **2024**, *16*, 4796. [CrossRef]
13. Li, X.; Liu, C.; Gou, K.; Yang, H.; Ren, X.; Peng, B. Effects of residual double bonds on the catalytic activity and stability of Pt/SDB hydrophobic catalysts. *RSC Adv.* **2015**, *5*, 45420–45425. [CrossRef]
14. Hu, S.; Hou, J.; Xiong, L.; Weng, K.; Ren, X.; Luo, Y. Preparation and characterization of hydrophobic Pt–Fe catalysts with enhanced catalytic activities for interface hydrogen isotope separation. *J. Hazard. Mater.* **2012**, *209*, 478–483. [CrossRef] [PubMed]
15. He, J.; Wang, H.; Xiao, C.; Li, J.; Chen, P.; Hou, J. Preparation and performance of Pt/PTFE/Foam SiC as a hydrophobic catalyst for LPCE. *Fusion Eng. Des.* **2016**, *113*, 269–274. [CrossRef]
16. Lu, Z.; Li, J.; Fu, X.; Hou, J.; Ran, G.; Xiao, C.; Wang, X. Superhydrophobic Pt@SBA-15 catalyst for hydrogen water isotope exchange reactions. *Int. J. Hydrogen Energy* **2022**, *47*, 18080–18087. [CrossRef]
17. Ruan, H.; Hu, S.; Hu, Z.; Zhang, L.; Dou, Q. Reaction Process on the Liquid Catalytic Isotopic Exchange of $H_2O$-$H_2$. *At. Energy Sci. Technol.* **2005**, *39*, 218–221.
18. Yamanishi, T.; Okuno, K. *A Computer Code Simulating Multistage Chemical Exchange Column Under Wide Range of Operating Conditions*; JAERI-DATA/CODE-96-028; Japan Atomic Energy Research Institute: Tokyo, Japan, 1996.
19. Ye, L.; Luo, D.; Tang, T.; Yang, W.; Yang, Y. Hydrogen isotope separation in hydrophobic catalysts between hydrogen and liquid water. *Fusion Eng. Des.* **2015**, *100*, 576–580. [CrossRef]
20. Zhang, Y.-B.; Liu, Q.; Shi, X.-C. Thermal Safety Study of Emulsion Explosive Matrix under the Coupled Effects of Environmental Pressure and Bubble Content with Internal Heat Source. *Processes* **2024**, *12*, 1677. [CrossRef]
21. Ji, L.; Si, Y.; Liu, H.; Song, X.; Zhu, W.; Zhu, A. Application of orthogonal experimental design in synthesis of mesoporous bioactive glass. *Microporous Mesoporous Mater.* **2014**, *184*, 122–126. [CrossRef]
22. Li, P.; Guo, L.; Xiong, R.; Luo, J.; Wen, M.; Yao, Y.; Zhang, Z.; Song, J.; Shi, Y.; Tang, T. Separation process study of liquid phase catalytic exchange reaction based on the Pt/C/PTFE catalysts. *Chin. J. Chem. Eng.* **2019**, *27*, 1837–1845. [CrossRef]
23. Li, J.; Kang, Y.; Ruan, H.; Dou, Q.; Han, Y.; Hu, S. Research on the Hydrogen-water Isotope Exchange Reaction by Pt-SDB Hydrophobi Catalyst. *At. Energy Sci. Technol.* **2002**, *36*, 125–128.
24. Fedorchenko, O.A.; Alekseev, I.A.; Bondarenko, S.D.; Vasyanina, T.V. Experimental Results and Experience with the LPCE Process. *Fusion Sci. Technol.* **2020**, *76*, 341–346. [CrossRef]